LAWRENCE
LIVERMORE
NATIONAL
LABORATORY

UCRL-CONF-221161

Thomson scattering techniques in laser produced plasmas

D. H. Froula, J. S. Ross, L. Divol, A. J. MacKinnon, C. Sorce, S. H. Glenzer

May 6, 2006

High Temperature Plasma Diagnostics
Williamsburg, VA, United States
May 7, 2006 through May 11, 2006

Thomson scattering techniques in laser produced plasmas

D. H. Froula, J. S. Ross, L. Divol, A. J. MacKinnon, C. Sorce, and S. H. Glenzer

Lawrence Livermore National Laboratory, University of California,

P.O. Box 808, Livermore, California 94551

Abstract

Thomson scattering has been shown to be a valuable technique for measuring the plasma conditions in laser produced plasmas. Measurement techniques are discussed that use the ion-acoustic frequency measured from the collective Thomson-scattering spectrum to extract the electron temperature, ion temperature, plasma flow, and electron density in a laser produced plasma. In a recent study, we demonstrated a novel Thomson-scattering technique to measure the dispersion of ion-acoustic fluctuations that employing multiple color Thomson-scattering diagnostics. We obtained frequency-resolved Thomson-scattering spectra of the two separate thermal ion-acoustic fluctuations with significantly different wave vectors. This new technique allows a simultaneous time resolved local measurement of electron density and temperature. The plasma fluctuations are shown to become dispersive with increasing electron temperature. Furthermore, a Thomson-scattering technique to measure the electron temperature profile is presented where recent experiments have measured a large electron temperature gradient (Te=1.4keV to Te=3.2 keV over 1.5-mm) along the axis of a 2-mm long hohlraum when heated asymmetrically.

PACS numbers:

I. INTRODUCTION

Thomson scattering measurements use an optical laser with a frequency (ω_o) and a wave number ($\mathbf{k}_o$) as a source that is elastically scattered by electron density fluctuations with wave vector $\mathbf{k}$. It was not until the advent of the laser [1] that there was sufficient luminous power to perform a successful Thomson-scattering experiment [2]; it can be shown that for typical laser plasmas, a laser intensity above 1×10^9 W-cm^{-2} is required to observe Thomson scattering above the background Bremsstrahlung emission [3]. Over the last 40 years, optical diagnostics have improved significantly allowing the application of Thomson scattering to extract fundamental plasma properties from the scattered frequency spectrum in a wide variety of plasmas in both magnetic fusion and inertial confinement fusion research.

Thomson scattering is used as a diagnostic to probe the individual electrons in the noncollective regime, and resonant plasma fluctuations in the collective regime [4–6]. Resonant electron plasma fluctuations ($\mathbf{k}_{epw}$) are observed when the light is scattered from electron density fluctuations with wavelengths larger than the Debye length ($\mathbf{k}_{epw}\lambda_{De} < 1; \lambda_{De} = \sqrt{\frac{\epsilon_o k_b T_e}{n_e e^2}}$). Collective ion-acoustic features ($\mathbf{k}_a$) are observed when the probed electrons follow the motion of the ions ($\mathrm{ZT}_e/\mathrm{T}_i > k_a^2\lambda_{De}^2$). In this regime the electrons move to screen the potential created by the ion fluctuations and the incident laser light is scattered from co- and counter-propagating ion-acoustic waves.

Ion-acoustic fluctuations provide the most intense features in the collective scattering spectrum and their frequency is commonly used to measure the electron temperature. In theory, the ion temperature can be obtained from the width of the intensity peaks in the Thomson-scattering spectra, but in laser-produced plasmas, velocity and temperature gradients within the scattering volume make this measurement unreliable. Adding a second ion species to the plasma introduces a second mode in the solution of the kinetic dispersion relation which can react quantitatively differently when the ion temperature is changed therefore, the ion temperature can accurately be extracted from the Thomson-scattering spectrum [7, 8]. Furthermore, observing light scattered in the collective regime from electron plasma waves ($\mathbf{k}_{epw}\lambda_{De} < 1$) provides a measure of the density [9–12], but the relatively small scattering signal requires a high-power probe laser or in the case of magnetic fusion plasmas a long integration time. A technique that simultaneously measures the local electron temperature and density using the dispersion of ion-acoustic fluctuations has recently

been presented [13].

In this paper, we will focus on Thomson-scattering techniques that allow measurements of the low frequency fluctuations in the collective regime where an accurate determination of the the local electron temperature, ion temperature, ion flow velocity, and electron density in laser produced plasmas.

II. BASIC THEORY

The Thomson-scattered power, P_s, into a solid angle $d\Omega$ per frequency range $d\omega$ is given by [3, 14],

$$\frac{dP_s}{d\Omega d\omega} = \hat{\eta}_1 \cdot \hat{\eta}_2 I_o r_o^2 \int dx S(k,\omega;x) n_e(x) \tag{1}$$

where $\hat{\eta}_i$ $(i = 1, 2)$ are polarization vectors defining the directions of the electric field of the Thomson probe and of the direction of the scattered light; $r_o^2 = e^2/m_e c^2 = 6.65 \times 10^{-25}$ cm^2 and I_o is the incident laser intensity.

The power spectrum for thermal density fluctuations in a plasma can be expressed using a theoretical form factor [15]:

$$S(k_a,\omega_a) = \frac{2\pi}{k_a}\left|1 - \frac{\chi_e}{\epsilon}\right|^2 f_e\left(\frac{\omega_a}{k_a}\right) + \frac{2\pi Z}{k_a}\left|1 - \frac{\chi_i}{\epsilon}\right|^2 f_i\left(\frac{\omega_a}{k_a}\right) \tag{2}$$

where $\epsilon(\omega_a, k_a) = 1 + \chi_e + \chi_i$ is the plasma dielectric function. In a Maxwellian plasma, the phase velocity ($v_\phi = \frac{\omega_a}{k_a}$) for low frequency ion-acoustic fluctuations is in the tail of the ion distribution function ($f_i(\frac{\omega_a}{k_a} >> v_\phi) \sim 0$) and near the peak of the electron distribution function ($f_e(\frac{\omega_a}{k_a} << v_\phi) \sim 1$), therefore, Eq. 2 is dominated by the first term on the right hand side. The frequency of the resonant fluctuations that are observed in the Thomson-scattering spectrum will be near the point where $\epsilon = 0$.

The ion-acoustic scattering wave vector is determined by energy and momentum equations:

$$\mathbf{k_a} = \mathbf{k_o} - \mathbf{k_s}$$

$$\omega_a = \omega_o - \omega_s.$$

When scattering from low-frequency fluctuations ($\mathrm{k}_o \simeq \mathrm{k}_s$), the acoustic wave vector is given by the experimental geometry and wave number of the probe laser,

$$k_a = 2k_o \sin\left(\frac{\theta}{2}\right) \tag{3}$$

where θ is the angle between the Thomson-scattering probe and the collection optics (Fig. 1). In this scattering regime ($\mathrm{ZT}_e/\mathrm{T}_i > k_a^2\lambda_{De}^2$), two ion-acoustic features can be observed in the scattered spectrum; the light is scattered by co- and counter propagating ion-acoustic waves ($\omega_a = \pm \mathrm{c}_s k_a$) in the plasma. The wavelength separation between the two ion-acoustic features is given by,

$$\frac{\Delta\lambda}{\lambda_o} = 4\sin\left(\frac{\theta}{2}\right)\sqrt{\frac{k_b T_e}{M}\left(\frac{Z}{(1+k^2\lambda_{De}^2)} + \frac{3T_i}{T_e}\right)} \tag{4}$$

where k_b is Boltzmann's constant, M is the ion mass, Z is the average charge state, and T_e and T_i are the electron and ion temperatures, respectively. This formula is used to illustrate the basic dependance of the scattering spectrum, but the kinetic form factor (Eq. 2) is used to fit the measured spectrum when a more accurate determination of the plasma parameters is desired.

III. EXPERIMENTAL DESIGN

A. Setup

Figure 1 shows a typical Thomson-scattering system; a lens collects and collimates the light scattered by the plasma. The collimated light is transported (often over several meters) to a lens that focuses the light into a spectrometer. In general, a high resolution spectrometer is required to resolve the ion-acoustic features; for a typical fully ionized nitrogen plasma (T_e = 1 keV, $T_e/T_i = 3$, $\mathrm{n}_e = 10^{20}$ cm^{-3}, Z=7) and a scattering angle of $\theta = 90^o$, Eq. 4 gives the separation between the ion-acoustic features of $\Delta\lambda/\lambda_o = 2.5 \times 10^{-3}$. To resolve this separation, our systems typically use a 1-meter f/8.7 Acton (Model AM-510) imaging spectrometer with a 3600 lines/mm grating (110 mm $\times$110 mm) and a d= 200 μm entrance slit width which results in a resolution of $\Delta\lambda/\lambda_o = 1.5\times10^{-4}$. The spectrum can be recorded using two configurations; imaging Thomson scattering uses a CCD (charge coupled devise) to measure the time integrated profile of the Thomson-scattering spectrum along the probe beam, while streaked Thomson-scattering employees a streak camera to record the temporal evolution of the scattered signal from a small volume in the plasma. In our systems, imaging Thomson-scattering (ITS) data are recorded with a gated intensified Princeton Instruments 16-bit CCD camera (PI-MAX) while our streak Thomson-scattering (STS) data use a high

dynamic range Hamamatsu streak camera (C7700) typically with a s= 150 μm temporal slit width. Both systems have comparable sensitivities; at $\lambda_o = 260$ nm the sensitivity of the CCD camera is $\gamma = 10^{-14}$ counts/J.

The temporal resolution of this system is limited by the spectrometer which can be calculated by the ray path difference across the grating; $\Delta\tau = \eta m \lambda_o / c$ where η is the number of grooves illuminated, m is the spectral order, and c is the speed of light, $\Delta\tau(\lambda_o = 260\text{ nm}) = 350$ ps.

B. Optics

The focal lengths of the collection and focusing lenes are chosen to maximize the coupling through the system and to determine the size of the Thomson-scattering volume (V_{ts}). To maximize the coupling through the spectrometer, the f-number of the focusing lens (f_{focus}) is chosen to be comparable with the f-number of the spectrometer. The Thomson-scattering volume is determined by the beam waist of the probe laser and the projection of the streak camera slit into the plasma plane (Fig. 1); the width of the spectral and temporal slits in the plasma plane are determined by the magnification of the system given by the ratio of the f-numbers of the lenes ($M \simeq \frac{f_{col.}}{f_{focus}}$). Typically our probe lasers have a ~ 60 μm diameter beam waist and a $f_{col.}/5$ collection lens is used in connection with a $f_{focus}/10$ focusing lens defining a cylindrical volume, $V_{ts} = \pi(30\ \mu\text{m})^2 \times 75\mu\text{m}$. Minimizing the Thomson-scattering volume reduces the spectral broadening by gradient effects and defines a precise location in the plasma.

The measured Thomson-scattering spectrum is broadened by the range of ion-acoustic waves probed ($\delta\omega_a$). When measuring a thermal scattering spectrum, this broadening can be calculated from Eq. 3 to be,

$$\frac{\delta\omega_a}{\omega_a} = \frac{\delta\lambda}{\Delta\lambda/2} = \frac{1}{4\tan\theta/2}\left(\frac{1}{f_{col.}} + \frac{1}{f_{probe}}\right).$$

For scattering with a 4ω ($\lambda_o = 265$ nm) probe laser from a typical fully ionized nitrogen plasma ($T_e = 1$ keV, $T_e/T_i = 3$, $n_e = 10^{20}$ cm^{-3}, Z=7) at a scattering angle of $\theta = 90^o$ and the optical configuration discussed above, the spectral smearing resulting from the optics is $\delta\omega_a/\omega_a = 0.1$ of half the total wavelength shift given by Eq. 4, $\delta\lambda = 0.07$ nm; this is comparable to the instrument function of the spectrometer, $\Delta\lambda = 0.04$ nm. Notice that, in

our system the resolution can be improved by a factor of two by increasing the f-number of the collection lens; this would reduce the scattered signal by a factor of 2, but to improve the resolution by another factor of two would require both a reduction in the spectral slit and an increase in the combined f-numbers therefore, reducing the scattering signal by a addition factor of 8.

C. Optical Alignment

One of the most critical aspects of a successful Thomson-scattering measurement is optical alignment. The projection of the instrument slits into the plasma must over lap the incident probe beam typically requiring alignment precision better than 50 μm. Our systems are aligned using ~ 100 μm spheres accurately positioned to the location of the desired Thomson-scattering volume. A low power alignment laser, operating at the same frequency as the probe beam, is used to back light the alignment ball. With the diagnostic slits open, an image of the ball is then projected through the spectrometer and onto the Thomson-scattering detector. Using the transport mirrors the ball is centered in between the slits, they are closed around the ball. The probe laser is aligned to the ball. It is often necessary to perform this final alignment under vacuum.

D. Probe Laser

[Discussion about narrow coherence, pulse width]

For a given experimental arrangement, the required probe laser energy can be estimated give the desired detector output (ITS and STS) necessary to achieve the optimal amplitude and signal-to-noise (S/N) ratio. There are three criteria that are considered when selecting the necessary laser power; number of other beams in the experiment, Bremsstrahlung radiation, and detector sensitivity.

Integrating Eq. 1 over the ion-acoustic features in the collective regime relates the probe laser energy (E_o) to the scattered energy (E_s) at $\theta = 90^o$,

$$E_s = \frac{1}{8f_{col.}^2} r_o^2 n_e L E_o. \tag{5}$$

where L is the length of the Thomson-scattering volume along the direction (axis) of the probe laser. For a beam diameter ϕ, optical magnification M= f_{col}/f_{focus}, the scattering

fluence at the spectrometer entrance slit is:

$$\Phi_s = \frac{E_s}{M^2 L \phi} \tag{6}$$

At the detector plane, for an entrance slit width d $\sim$ Mϕ and optical transmission T, the scattered fluence is imaged as two peaks of width d (separation=$\Delta\lambda$) and can be equated to the detector fluence;

$$\Phi_d = \frac{E_s \mathrm{T}}{2\mathrm{d\ L\ M}} = \frac{N}{\sigma\gamma} \tag{7}$$

where N is the average number of counts in the spectral peaks detected over the probe laser pulse by a single pixel of area σ and sensitivity γ (counts/J).

Equations 5 and 7 yield the required probe laser energy required for the (time integrated) imaging spectrometer system (ITS).

$$E_o^{ITS} = \frac{16 f_{col}^2}{r_o^2 n_e} \frac{N}{\sigma\gamma} \frac{dM}{T} \tag{8}$$

The laser energy required for the streaked spectrometer system (STS) is,

$$E_o^{STS} = E_o^{ITS} \frac{\Delta t}{\Delta T} \tag{9}$$

where ΔT is the temporal slit width and Δt is the pulse width of the laser probe. Table I is a compilation of successful Thomson-scattering experiments with a variety of configurations.

IV. EXPERIMENTAL TECHNIQUES TO MEASURE PLASMA CONDITIONS

A. Electron Temperature

An experiment to measure the electron temperature in the blow-off plasma from a Au sphere heated with 59 3-ns frequency trippled laser beams at the Omega Laser Facility is shown. The 4ω Thomson probe laser employed x J to produce an average detector signal of N=x. The electron temperature was determined by fitting Eq. 2 to the spectrum assuming that the average charge state for Au is Z= $45T^{0.2}$ [**?**].

The sensitivity of the fit to electron temperature is shown in Fig. 3 where the electron temperature is varied by 20% around the best fit $\mathrm{T}_e = 1\ keV$ while all other parameters where kept fixed.

Figure 4 shows a Thomson-scattering spectra collected along the axis of a CH-gas-filled hohlraum uniformly heated by 33 ultra-violet laser beams with a total energy of 15 kJ.

The electron temperature profile is extracted by fitting Eq. 2 to the measured spectra. Figure **??** shows the sensitivity of the electron temperature to the separation of the ion-acoustic features through a series of calculated spectra where the electron temperature is varied from $T_e = 2.8$ keV to $T_e = 3.2$ keV while keeping all other parameters fixed ($T_i = 2$ keV, $n_e = 6 \times 10^{20}$ cm^{-3}).

B. Ion Temperature

Adding a second ion species to the plasma introduces a second mode in the solution to the kinetic dispersion relation which reacts qualitatively differently when the ion temperature is changed. Namely, when the ion temperature is increase, the damping of the two modes moves inversely. Therefore, the relative damping of the modes provides an accurate measure of the ion temperature which is observed in the scattering amplitude of the ion-acoustic features [7, 8].

The scattering spectrum shown in Figure 5 demonstrates the change in relative damping of the two modes in a multi-ion carbon-hydrogen plasma. Early in time, the hydrogen-like mode is dominant; in the series of spectra that are shown in Figure 5(b-f) the carbon-like mode grows in time indicating an increase in the ratio between the ion and electron temperature. As the ion temperature equilibrates with the laser heated electrons, the carbon-like mode becomes evident and is dominant by the end of the scattering experiment. Fitting the data with the Thomson-scattering form factor for a two-ion-species plasma [16] accurately measures the electron temperature and ion temperature in the CH plasmas.

C. Electron Density

Measuring the electron density in laser produced plasmas is challenging. In the past, density measurements have primarily been inferred using spatially integrated measurements: stimulated Raman scattering [17], interferometry, and spectroscopy [18].

Thomson-scattering provides a unique way of measuring the density; the ability to define a small scattering region allows the only viable local measure of density in a laser produced plasma. In theory, there are three independent ways to measure the density using Thomson scattering: measuring the scattered power, measuring the frequency of the electron plasma

wave, and measuring the ion-acoustic dispersion.

In magnetic fusion experiments, the sensitivity of the Thomson-scattering systems are commonly absolutely calibrated using Rayleigh scattering to provide a measure of the electron density from the scattered power. Although this technique has been used in laser produced plasmas [12], it is significantly more challenging to perform using a single shot high power laser system and requires significant dedicated target chamber center time which is often unavailable at large laser facilities.

Measuring the electron plasma fluctuations [9–11, 19] provides a direct measure of the electron density, but the relatively small scattered signal makes this measurement challenging and requires a high-power probe laser [9]. Recently a new technique for measuring density using the ion-acoustic features has been presented [13] allowing standard low power probe lasers to be employed ensuring that the plasma conditions are not perturbed. This technique exposes the fact that the dispersion of ion-acoustic waves are sensitive to the Debye shielding in high temperature plasmas.

1. Scattered Power

From Eq. 1 it is evident that the scattered power is a function of the electron density; Figure 6 shows the relative electron density variation extracted from the intensity of the scattered light presented in Figure 5. By scaling the scattered power measurement at 400 ps to the initial gas fill density $n_e = 5.7 \times 10^{20}$ cm^{-3} (assuming a fully ionized plasma and no early time hydrodynamic motion), the measured density evolution is determined by fitting Eq. 1 to the measured spectra.

2. Ion-Acoustic Dispersion

In high temperature plasmas, the frequency of ion-acoustic fluctuations are sensitive to both the electron temperature and density. The use of multiple Thomson-scattering diagnostics allow the measure of the local frequency of the ion-acoustic fluctuations for large and small wave vectors. The dispersion of ion-acoustic fluctuations with large wave numbers are sensitive to Debye shielding ($k_a \lambda_{De} > 1$). This technique has been shown to be a powerful diagnostic of both the local electron density and local electron temperature with

high temporal and spatial resolution [13], and could be applied for a variety of applications across the fields of plasma physics where other diagnostics have failed to provide accurate measurements.

The advantage of applying two spectrometers measuring the ion-acoustic waves in the Thomson-scattering spectrum is the fact that these fluctuations provide the most intense features in the collective scattering spectrum and their frequency spectrum is a proven signature for measurements of the electron temperature at both large and small laser facilities. This technique employs one detector to measure the ion acoustic frequency for small k-vector fluctuations providing the electron temperature while the second detector measures the acoustic frequency for large k-vector fluctuations providing the electron density from the $\mathrm{k}_a\lambda_{De}$ correction in the dispersion relation illustrated in Eq. 4.

The two ion-acoustic frequencies can be measured by either using two probe wavelengths or a single probe laser with two significantly different scattering angles. A small angle diagnostic (k_a^1) can be chosen to provide a good measure of the electron temperature with a small dependence on the density ($k_a^1\lambda_{De} < 1$) while a large angle diagnostic (k_a^2) would provide a good measure of the electron density ($k_a^2\lambda_{De} > 1$). There is a limitation for large angles (for a given probe wavelength) given by the constraint of remaining in the collective Thomson-scattering regime ($\frac{ZT_e}{T_i} >> k_a^2\lambda_{De}^2$) while there is a practical limit for small angles given by the instruments ability to resolve the spectral peaks (i.e. the wavelength separation scales with the angle as seen in Eq. 4).

For a typical inertial confinement fusion plasma ($T_e = 5$ keV, $n_e = 5 \times 10^{20}$ cm^{-3}) the optimal scattering angles for the two collection optics are $40^o < \theta_{k2} < 80^o$ ($0.4 < k_2\lambda_{De} < 0.7$) and $\theta_{k_1} > 140^o$ ($k_1\lambda_{De} > 0.9$); using these scattering angles, a single 4ω probe laser, and typical instrument resolutions, the local density could be measured to better than 25% with an electron temperature measurement to within 10%.

V. STUDY OF LASER DRIVEN PLASMA WAVES

The unique ability for Thomson-scattering to probe a defined wave vector allows the investigation of laser driven instabilities [20]. For example, stimulated Brilloin scattering (SBS) is a three wave instability that results from the resonant coupling of an intense laser pulse (k_{IB}), a scattered light wave, and an ion-acoustic plasma wave (k_{driven}). The process is

resonant for a given ion-acoustic wave co-propagating to the incident interaction beam (IB). It is evident that the specific ion-acoustic waves can be probed by selecting a scattering geometry consistent with Eq. 3; for SBS driven ion-acoustic waves ($k_{driven} = 2k_{IB}$) the geometry is given by:

$$\sin\left(\frac{\theta}{2}\right) = \frac{k_{IB}}{k_{ts}}$$

where $\mathrm{k}_{ts} = \frac{2\pi}{\lambda_{ts}}$ and λ_{ts} is the wavelength of the probe laser.

Using Thomson-scattering to scatter from the driven ion-acoustic waves and the counter-propagating thermal fluctuations, the absolute amplitude of the driven ion-acoustic wave has been measured [21]. The absolute amplitude of the driven ion-acoustic wave ($\frac{\delta n}{n_e}$) is measured by comparing the scattered power from thermal fluctuations, with the power scattered by the driven acoustic wave (Bragg scattering) which gives the ratio [17]

$$\frac{P_{driven}}{P_{thermal}} = \frac{\pi n_e \lambda_o^2 L_c}{2f}\left(\frac{\delta n}{n_e}\right)^2, \tag{10}$$

where L_c is the correlation length of the driven ion-acoustic wave along the direction of the Thomson-scatter probe beam, f is the maximum f-number between the interaction beam and the collection optics. The correlation length can be estimated by the transverse size of speckles generated by the interaction beam $L_c = f_{IB}\lambda_{IB}$.

Combining this technique with a multi-ion species Be/Au plasma to measure the ion-temperature has shown direct quantitative evidence of hot ions created by trapping in low-Z laser plasmas [Fig. 7(a)] [8, 22]. Furthermore, by measuring the absolute frequency of the driven ion-acoustic waves Thomson-scattering was used to measure the frequency shift that results from the trapped ions [Fig. 7(b)] [23].

These measurements have been compared with laser-plasma interaction simulations which have shown that ion trapping is a mechanism for saturating the SBS instability in low-Z plasmas. Similar studies have been done in mid-Z ($Z > 4$) plasmas where trapping is unlikely to have an effect on the SBS process. A possible saturation mechanism for SBS in a mid-Z plasma is harmonic generation. Recently a study has measured the amplitude simultaneously of the primary SBS driven ion-acoustic wave ($2\mathrm{k}_{IB}$) and the secondary ($4\mathrm{k}_{IB}$) or tertiary ($6\mathrm{k}_{IB}$) wave **??**.

VI. CONCLUSIONS

Measuring the ion-acoustic features in the Thomson-scattering spectrum has been shown to be the only reliable measure of the plasma conditions in a laser produced plasma. We present several Thomson scattering techniques that rely only on measuring the frequency of the ion-acoustic features to extract the LOCAL electron temperature, ion temperature, plasma flow, and electron density. We present guidelines for configuring a Thomson-scattering system including a determining the necessary power in the probe laser.

This work was performed under the auspices of the U.S. Department of Energy by the Lawrence Livermore National Laboratory under Contract No. W-7405-ENG-48.

---

[1] T. H. Maiman, Nature **187**, 493 (1960).

[2] H. J. Kunze, E. Funfer, B. Kronast, and W. H. Kegel, Physical Review **11** (1964).

[3] D. E. Evans and J. Katzenstein, Rep. Prog. Phys. **32**, 207 (1969).

[4] B. S. Bauer, R. P. Drake, K. G. Estabrook, R. G. Watt, M. D. Wilke, and S. A. Baker, Phys. Rev. Lett. **74**, 3604 (1995).

[5] H. A. Baldis, D. M. Villeneuve, and C. J. Walsh, Can. J. Phys. **64**, 961 (1986).

[6] P. E. Young and K. G. Estabrook, Physical Review E **49**, 5556 (1994).

[7] S. H. Glenzer, C. A. Back, K. G. Estabrook, R. Wallace, K. Baker, B. J. MacGowan, B. A. Hammel, R. E. Cid, and J. S. D. Groot, Phys. Rev. Lett. **77**, 1496 (1996).

[8] D. H. Froula, L. M. Divol, and S. H. Glenzer, Phys. Rev. Lett. **88**, 105003 (2002).

[9] S. H. Glenzer, W. Rozmus, B. J. MacGowan, K. G. Estabrook, J. S. D. Groot, and G. B. Zimmerman, Phys. Rev. Lett. **82**, 97 (1999).

[10] E. Fourkal, V. Y. Bychenkov, W. Rozmus, R. Sydora, C. Kirkby, C. E. Capjack, S. H. Glenzer, and H. A. Baldis, Phys. Plasmas **8**, 550 (2001).

[11] S. C. Snyder, L. D. Reynolds, J. R. Fincke, G. D. Lassahn, J. D. Grandy, and T. E. Repetti, Physical Review E **50**, 519 (1994).

[12] G. Gregori, S. H. Glenzer, J. Knight, C. Niemann, D. Price, D. H. Froula, M. J. Edwards, R. P. J. Town, W. Rozmus, A. Brantov, et al., Phys. Rev. Lett. **92** (2004).

[13] D. Froula, P. Davis, L. Divol, J. Ross, N. Meezan, D. Price, S. Glenzer, and C. Rousseaux,

Phys. Rev. Lett. **95**, (2005).

[14] J. Myatt, Ph.D. thesis, University of Alberta (1997).

[15] J. A. Fejer, Can. J. Phys. **38**, 1114 (1960).

[16] D. E. Evans, Plasma Physics **12**, 573 (1970).

[17] D. H. Froula, L. Divol, D. G. Braun, B. I. Cohen, G. Gregori, A. Mackinnon, E. A. Williams, S. H. Glenzer, H. A. Baldis, D. S. Montgomery, et al., Phys. Plasmas **10**, 1846 (2003).

[18] C. DEMICHELIS and M. MATTIOLI, NUCLEAR FUSION **21**, 677 (1981).

[19] G. Gregori, J. Schein, P. Schwendinger, U. Kortshagen, J. Heberlein, and E. Pfender, Physical Review E **59**, 2286 (1999).

[20] S. H. Glenzer, L. M. Divol, R. L. Berger, C. Geddes, R. K. Kirkwood, J. Moody, E. A. Williams, and P. E. Young, Phys. Rev. Lett. **86**, 2565 (2001).

[21] D. H. Froula, Ph.D. thesis, University of California at Davis (2002).

[22] D. H. Froula, L. Divol, H. A. Baldis, R. L. Berger, D. G. Braun, B. I. Cohen, R. P. Johnson, D. S. Montgomery, E. A. Williams, and S. H. Glenzer, Phys. Plasmas **9**, 4709 (2002).

[23] D. H. Froula, L. Divol, A. A. Offenberger, N. Meezan, T. Ao, G. Gregori, C. Niemann, D. Price, C. A. Smith, and S. H. Glenzer, Phys. Rev. Lett. **93**, 35001 (2004).

Figures

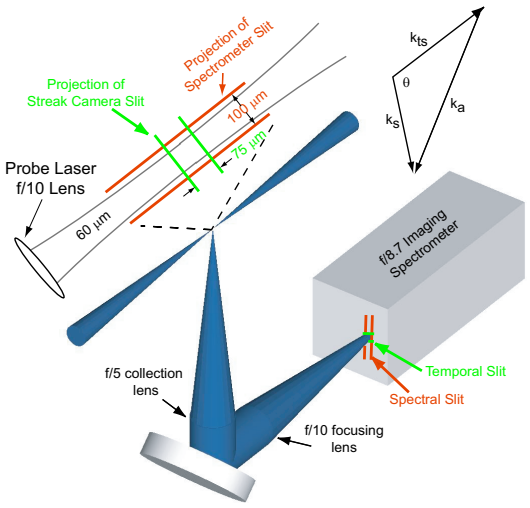

FIG. 1: A typical Thomson scattering setup is shown. The spectrometer and streak camera slits are imaged into the plasma plane defining the Thomson-scattering volume. The scattering vector diagram is shown.

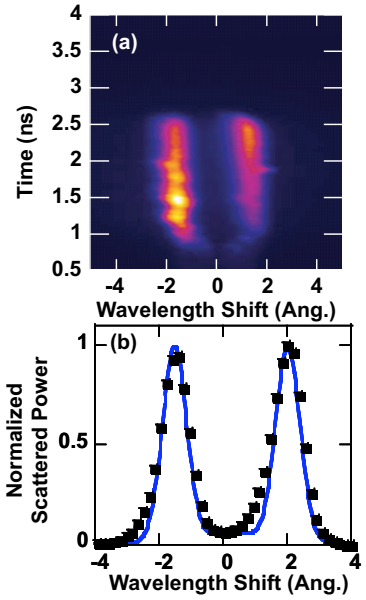

FIG. 2: (a) The Au Thomson-scattering spectrum is shown where the temporal evolution of the two ion-acoustic features are clearly observed. (b) The spectrum at 2 ns is fit with a theoretical form factor to give an electron temperature of $T_e = 1$ keV.

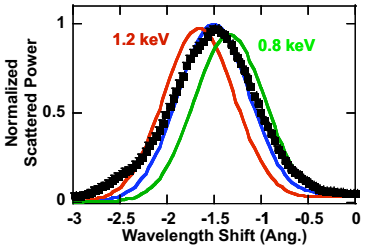

FIG. 3: The sensitivity of the spectral fit to the electron temperature is shown by varying the electron temperature by 20% around the best $T_e = 1$ keV fit.

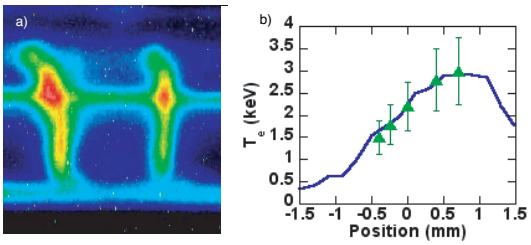

FIG. 4: (a)

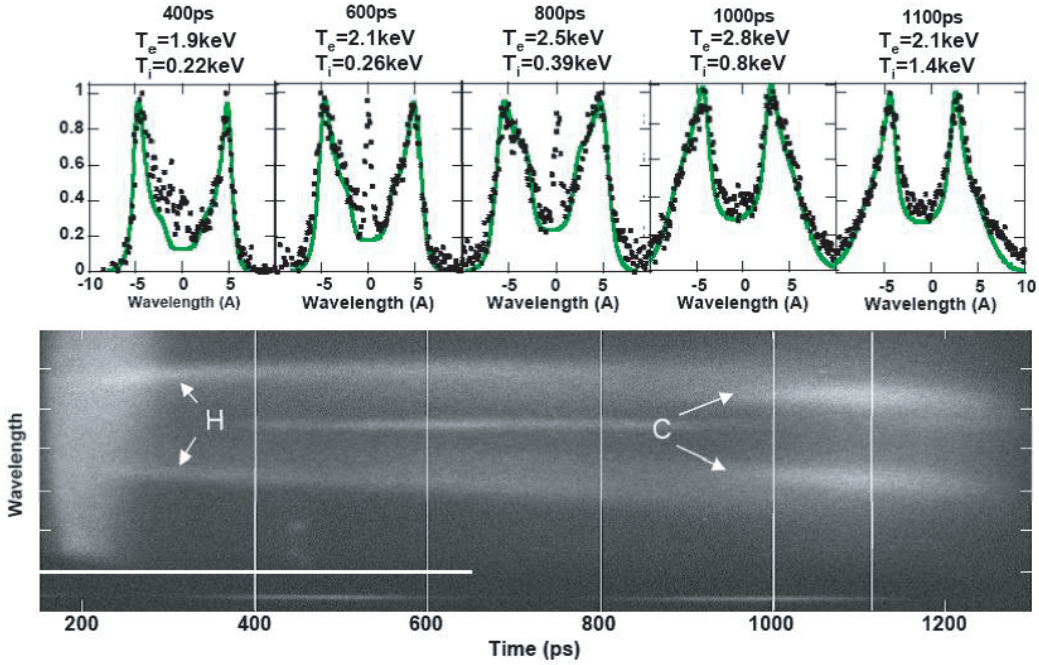

FIG. 5: (a) The streaked Thomson-scattering spectrum shows a heavily damped carbon-like mode and a weakly damped hydrogen-like mode early in time. The damping of the modes is reversed by the end of the probe beam. The spectra are fit to determine T_e, T_i, and n_e at selected times (b) 400 ps, (c) 600 ps, (d) 800 ps, (e) 1000 ps, (f) 1100 ps. The scattered light is collected from the center of a gas filled hohlraum.

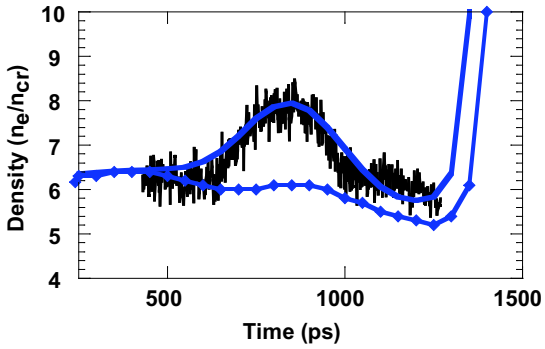

FIG. 6: The relative electron density evolution measured (black line) using the power collected in the Thomson-scattering diagnostic is compared with a hydrodynamic simulation for a CH-gas filled hohlraum with a total heater beam energy of 13.5 kJ.

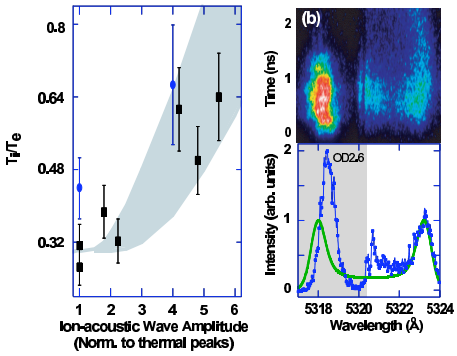

FIG. 7: (a) The ratio of T_e/T_i as a function of the normalized ion-wave amplitude shows evidence of the generation of hot ions and ion trapping in Be/Au plasmas. (b) A frequency shift is measured on the ion-acoustic wave driven by SBS; the solid line is the measured spectrum from a second Thomson-scattering diagnostic that is not effected by the SBS process. Half of the spectrum is filtered at the slit of the streak camera using an OD2.6.

Tables

System	Heaters	Target	n_e	ND	γ	E_o	f_{col}	d	s	σ	Δt	ΔT	λ_{ts}	N
	kJ		10^{19} cm^{-3}		cnts/J	J		μm	μm	cm^2	ns	ns	nm	counts
ITS	0.2	N_2 Jet	1.5	0	10^{14}	0.5	5	150	–	7×10^{-6}	0.2	–	527	7000

STS	0.2	N_2 Jet	1.5	0	?	1.0	5	200	200	$? \times 10^{-6}$	1.0	0.2	263	1500
STS	16	CH-GFH	60	1	?	150	10	200	200	$? \times 10^{-6}$	1.0	0.2	263	8000
STS	27	Au Sphere	60	1	?	150	10	200	200	$? \times 10^{-6}$	1.0	0.2	263	8000
STS	27	Au Sphere	60	0	?	15	10	200	200	$? \times 10^{-6}$	3.0	0.2	263	8000
STS	27	Au Sphere	60	0	?	100	10	200	200	$? \times 10^{-6}$	3.0	0.2	263	8000
STS	27	Au Sphere	60	0	?	150	10	200	200	$? \times 10^{-6}$	3.0	0.2	263	8000

TABLE I: The optical transmission on all of these systems is approximately T=0.2 and the magnification is M=2.